An Experimental test for cracking concrete under controlled conditions

C.Boulay[1], S.Dal Pont[1], A.Delaplace[2], H.Delahousse[1], J-L.Tailhan[1]
[1] *Division for Cement and Concrete Composites, French Public Works Research Laboratory, BCC-LCPC, Paris, France;*
[2] *LMT (ENS Cachan/CNRS/UPMC/PRES UniverSud Paris) Cachan, France*

1 Introduction

A satisfying description of the microstructure of an heterogeneous material such as concrete should take into account the presence of cracks. Indeed, their inevitable presence weakens the porous matrix resistance and constitutes a preferential flow path for fluid, gas and pollutants: material durability is therefore seriously affected. A proper numerical modeling of concrete subjected to severe loading conditions should take into account these phenomena: the description of the behavior of a cracked concrete studied as a multiphase porous media requires the definition of an experimental constitutive law relating the typical durability indicators (such as permeability/diffusivity/electrical resistivity) to the crack width.

A typical sequence of operations, in order to find the relationship between cracks and transfer properties, consists in: a first step where cracks are produced, a second step of geometrical description of the cracks and a third step leading to the characterization of transfer properties (resistivity, fluid permeability or ionic diffusivity) on residual cracks.

This paper deals with the feasibility of transfer properties measurement tests during the post-peak cracking phase of concrete. In such a case, parameters like chloride diffusivity or gas/water permeability exhibit a sharp increase which has been observed on pre-cracked concrete [1, 2, 5]. However, a proper description of the evolution of these properties should be monitored in real-time as cracks open in the specimen. In this paper, attention is focused on the mechanical test and the geometrical characterization of the cracks by means of a displacement measurement system together with a digital image correlation technique [6, 7].

Usually, mechanical tests used to explore the post-peak phase lead to distributed multiple crack patterns [1, 8, 9] or to single well-defined crack [2, 3, 4, 5]. The former geometry is obviously more difficult to characterize than the latter. Given our objective, tests leading to a unique crack were chosen. Direct tensile test, bending test or Brazilian test are good candidates but, with the aim of performing durability tests during and after the loading, the Brazilian splitting test has been retained.

2 Testing conditions

The mix proportions of the concrete used for the design of the tests is given in table 1. It is a classical concrete for bridges.

Components		**Mass (kg) / m^3**
Cement	: CEM I 52,5 N PMES CP2 / Lafarge / Le Havre	340
Water		184,22
Sand (river)	: Bernières 0/4	739,45
Gravels (river)	: Bernières 6,3/20	1072,14

Tableau 1: Mix design.

Cylinders with 100 cm² in cross section and 22 cm in height were cast in steel moulds for the sake of a good geometry. They were cured wrapped in an auto-adhesive aluminium tape. They were aged of more than three months at the time of the tests. Before the test, specimens were sliced and their faces were grounded to reach a thickness of 5 cm (three samples can be drawn from one cylinder).

Splitting tests were performed with a ± 500 kN hydraulic testing machine equipped with a feedback. The controlled variable can be either the displacement of the piston, measured by a 200mm LVDT, or the load measured by a load cell or an external parameter chosen by users. Calculated variable can also be chosen for feedback signal instead of a single channel. It consists of a real time mathematical combination of signals from individual measurement transducers. A lower bearing plate (fig. 1, ref. 1) is fixed at the top end of the piston (bottom of the testing machine) while the upper bearing plate is a part of a ball and socket joint (ref. 2) under the load cell (ref. 3). The sample (ref. 4) is loaded between these bearing plates.

As permeation tests or image correlation tests has to be performed, no displacement transducer can be fixed or glued on both ends of the specimen. Displacements are measured at each side of the horizontal diameter. As mentioned by [2] and [3], cracks generally open on one face before the other. Hence, two pairs of LVDTs (stroke = ± 1 mm, ref. 5) were maintained by a rigid frame (ref. 6) bearing on the lower plate of the machine, in order to measure the variations of two diameters. The frame is non deformable and its temperature sensitivity was measured. The distance (a) between the axis of the LVDTs can not be equal to the thickness (b) of the sample so a lower distance (3 cm) has been chosen. Tips of LVDTs were not directly in contact with the sample but with glass blades (ref. 7) glued on each side (axial displacements of each LVDTs are of the same order of magnitude than orthogonal displacements close to the tip of the transducers).

Ordinary adhesive tapes were placed on the bearing lines instead of using plywood or cardboard between sample and bearing plates of the machine. In that case, it is a much better choice to distribute the load because preliminary tests

with usual bearing devices showed that, even in the pre peak zone of the loading, displacements were not symmetrical.

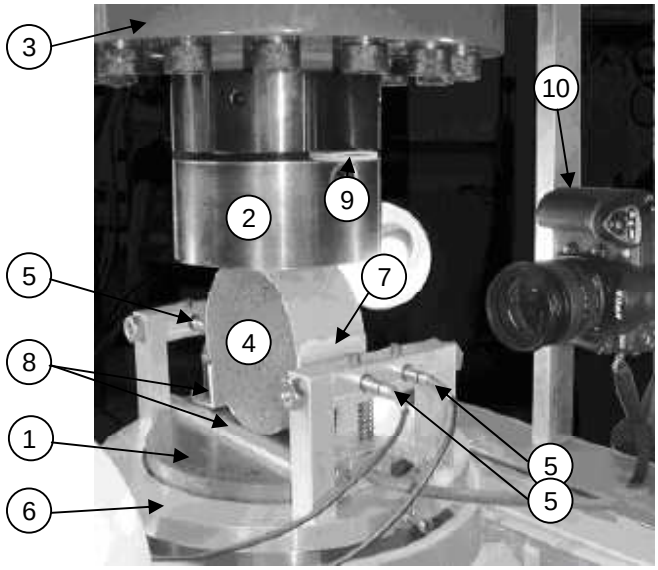

Figure 1: Test settings.

Samples are aligned and maintained on the lower plate with a special test rig (ref. 8) avoiding any displacement during the docking between the sample and the upper plate. During docking, the ball and socket joint rotates to counteract eventual out of parallelism of bearing lines. After docking, the lateral movement of the ball and socket joint is restrained by the means of compliant spacers (ref. 9) of equal thicknesses.

The four measured displacements are named (Δl_{fl}, Δl_{fr}, Δl_{rl}, Δl_{rr}) in function of the situation of the LVDTs on the testing machine: respectively the front left displacement, the front right, the rear left and the rear right. The sum of the front displacements gives the variations of the diameter 15 mm in front of the mid section ($\Delta Ø_{fm} = \Delta l_{fl} + \Delta l_{fr}$) while the sum of the rear displacements gives the variations of the diameter 15 mm backward ($\Delta Ø_{rm} = \Delta l_{rl} + \Delta l_{rr}$). The mean value ($\Delta Ø$) of these two variations, calculated by the testing machine in real time, becomes the control variable. The tuning of the closed loop (Proportional / Integral / Derivative actions) is delicate but possible with successive tests.

Two cameras (ref. 10) are fixed in front of the faces of the sample, with optical axis collinear with the axis of the sample.

The successive steps, during the test, were as follows. The first pictures are taken by the two cameras without loading. The docking is manual until a pre load of about 0.5 kN. A ramp is started at a rate of $\Delta Ø/dt = 10$ µm/mn and pictures are automatically taken at a rate of 4/mn. When the mean displacement reaches

100 µm, the ramp is reversed down to 83 µm. Then a loading rate of 5 kN/mn is applied to reach 2 kN. Then the sample is completely unloaded with the control on the displacement of the piston.

3 Experimental analysis of displacement transducers measurements

As there is always a dissymmetry between faces, results are expressed on both sides (rear and front) of the specimen.

The analysis of diameter variations (fig. 2 left) shows similar measurements in the pre peak zone. It confirms that bearing conditions are suitable when the sample is still elastic. Differences between rear and front measurements are shown in the post peak period. It confirms the necessity of a control on the mean value of the displacements. A zoom (figure 2 right) on this curve indicates, three times, that the displacement on one face snaps back (arrows) while, on the other face, the displacement increases. A control with only one measurement would have failed because of these quick recoveries.

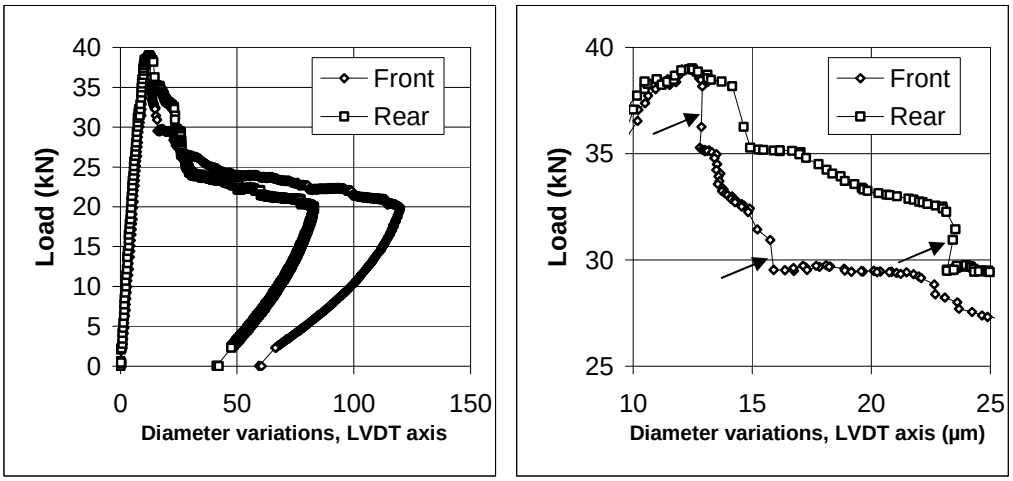

Figure 2 : Diameter variations are obtained by summing front displacements on one hand, and rear displacements on the other hand.

The crack opening displacement (COD) is calculated from measured displacements in two steps.

The first step of the calculation consists of determining which would have been the diameter variation on each face of the sample (figure 3 left) instead of measuring the displacements in the axis of LVDTs. For this purpose, it is supposed that plane sections remain plane. This calculation emphasizes the discrepancy between the rear and the front face after the peak load. The amplitude of the snap-backs on each side is more important.

The second step consists to remove the elastic part of these variations (figure 3 right) provided that, after the peak load, the sample is split into two elastic blocks without damaged zones on the lips of the crack. The elastic part is a function of the load, deduced of the pre peak slope of the curve obtained in the first step.

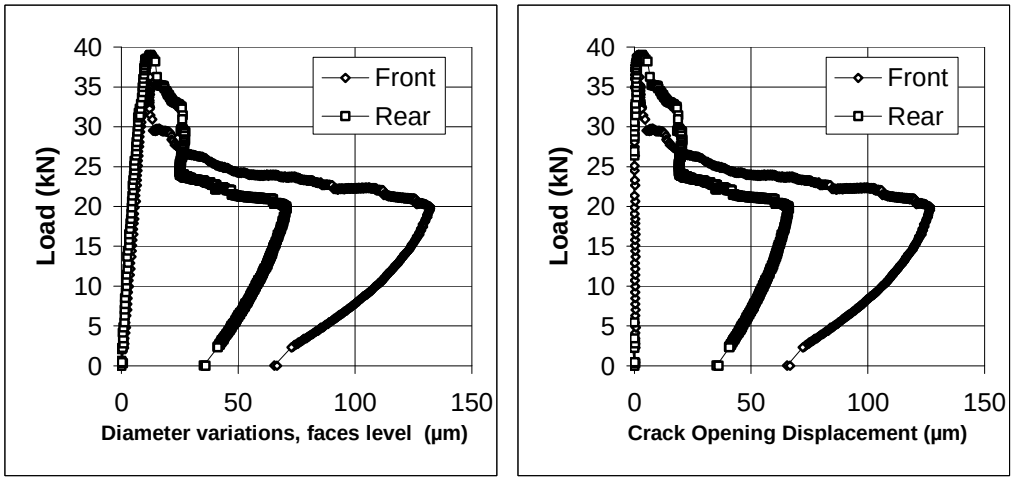

Figure 3 : Diameter variations on the faces of the sample and COD at mid height.

The figure 3 (right) shows that the front COD goes faster, just after the peak load, than the rear COD which is quasi stopped. At about 19 µm for the front COD, the crack stops to increase and snaps back while the rear COD starts to increase.

This mechanism, also observed on other samples, illustrates that one side is (always) weaker than the other. The crack propagates from this side to the other in the first few micrometers of COD. During the further crack opening, frictions through the crack, between aggregates and matrix, are involved in the opening mechanisms. These frictions are attributed to autogenous shrinkage of the cement paste restrained by the aggregates [10, 11]. This mechanism should be taken into account in numerical modelling (a full 3D analysis is necessary). The area of the crack is also pertinent in numerical modelling but this dimension is missing in the previous measurements. That's why another technique is used for a field characterization.

4. Experimental analysis with digital image correlation (DIC)

Digital image correlation (see for example [12], [13]) has been used on both sample faces in order to obtain a full displacement field and a fine description of the crack. Basically, the displacement field is obtained from two pictures taken at two different loading levels. Calling respectively $f(\mathbf{x})$ and $g(\mathbf{x})$ the grey level distributions of the reference image and the deformed one, the displacement field $\mathbf{u}(\mathbf{x})$ is gained as $g(\mathbf{x}+\mathbf{u}) = f(\mathbf{x})$. As the displacement is not homogeneous on the sample, the image is subdivided into regions of interest (ROIs), and the displacement is computed on each ROI. The analysis proposed here is an

enhanced version of this principle, where a sub-pixel algorithm is introduced based on a Q4-interpolation of the displacement field [13]. Two kinds of analysis are performed:

- the first one corresponds to a simple « tracking », where just a local displacement value is computed. It allows a comparison of the results obtained with the four LVDTs and with DIC.

- the second one uses the computation of the full displacement field, and gives the crack pattern as well as the main crack opening value.

Two Nikon D200 cameras are used for the experiment. Each image resolution is 2616x3900 pixels. The physical size of a pixel is 0.05 mm.

4.1 Local displacement measure

In this part, the left and right displacements of the front and rear faces are computed. The regions of interest (ROIs) are shown on figure 4 (squares of 256x256 pixels).

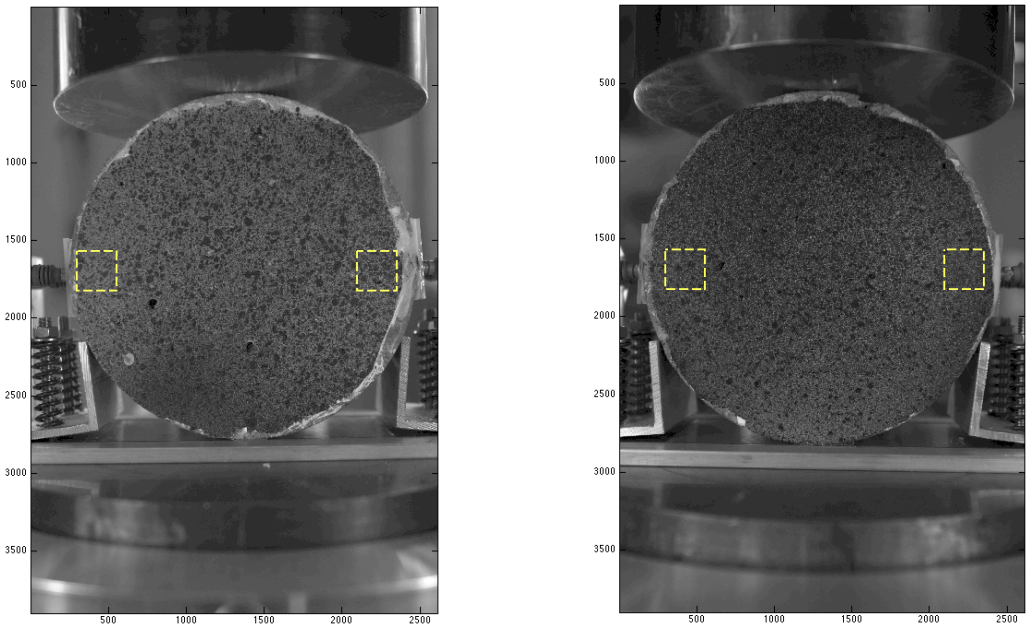

Figure 4: ROIs for the front side (left) and the rear one (right).

50 pictures for each side are analyzed. Figure 5 shows the comparison of the measurement between LVDTs and DIC for the front side. As expected, a good agreement is observed and proves the reliability of the measure by DIC. One can note a divergence in measurements concerning the right displacement after the

unloading. This difference can be explained considering that the measured points are not the same for both techniques.

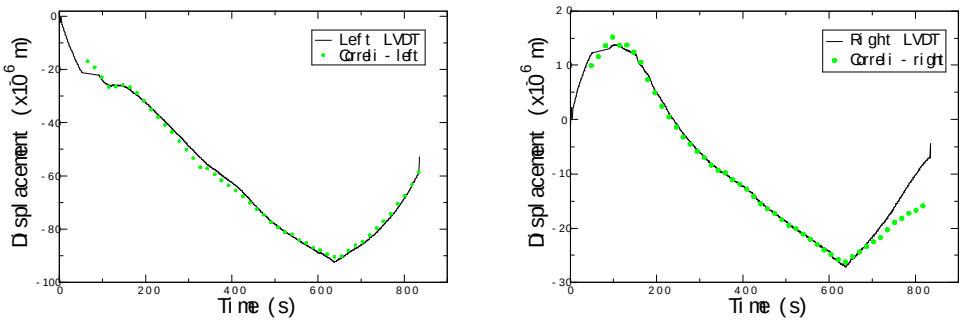

Figure 5: Comparison of the left (left) and right (right) displacement measurements for the front side.

4.2 Displacement field and crack pattern analysis

We propose in this part to compute the central displacement field (the region where the crack is expected to appear). Figure 6 shows the results for the ROIs for both faces at the end of the loading. The color scale is in pixel. As for the lateral displacement, an asymmetry of the crack pattern as well as the opening value is clearly visible, due to the strong heterogeneity of the concrete.

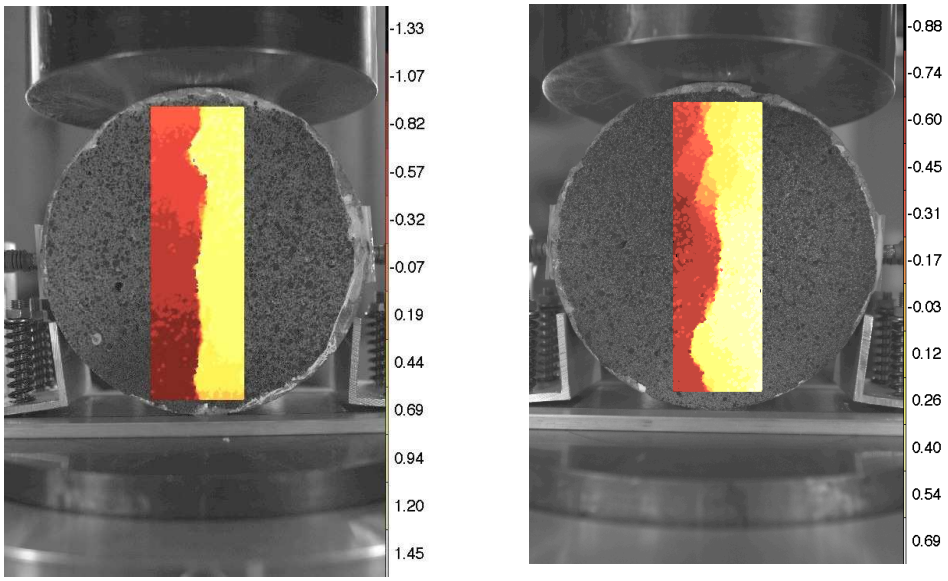

Figure 6: Crack pattern for the front side (left) and the rear one (right).

The main information obtained from these displacement fields is the crack pattern all along the loading. Hence, the nucleation and the propagation of the central macro-crack in the sample can be observed. Considering an elastic behavior outside of the crack, one can compute the crack opening value all along the loading process, by choosing two relevant ROIs on each side of the crack. This analysis is shown, for the front face, by figure 7 (left). A comparison with the approximation obtained from the LVDTs measurement (see fig. 3 right) gives again a good agreement. An extra output allowed by DIC is the value of the crack opening all along the sample height. The displacements of the left crack lip and the right one are plotted on figure 7 (right) for the maximum displacement. The horizontal box represents the location of the measurements plotted on the left graph.

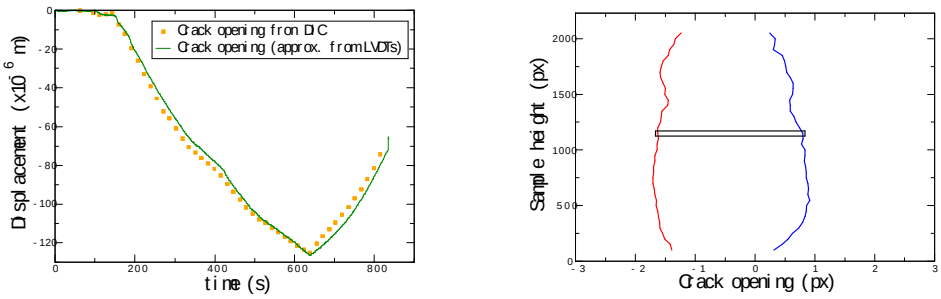

Figure 7: Crack opening for the front side.

5 Conclusion

In order to prepare transfer properties tests on cracked concretes under loading, a displacement controlled splitting test has been designed. This test gives COD derived from diameter variations measurements done by LVDTs at mid height of the cylindrical sample.

The comparison between this COD and results from digital image correlation technique is in a good agreement. This DIC method allows the calculation of the COD all along the path of the crack. It is then possible to give the area of the crack on both sides of the specimen. The correlation between the crack width and transfer properties is then completed.

As it is not possible to take pictures associated with DIC method while a transfer test is in progress, it is planned to obtain a function giving a mean crack area vs. the COD obtained with LVDTs and the position along the crack path, after a series of splitting test on samples made of the same concrete.

6 References

[1] Saito M., Ishimori H., "Chloride permeability of concrete under static and repeated compressive loading", *Cement and Concrete Research*, Vol. 25, n° 4, 1995, pp 803-808.

[2] Wang K., Daniel C. Jansen, Surendra P. Shah, Alan F. Karr, "Permeability study of cracked concrete", *Cement and Concrete Research*, Vol. 27, No. 3, pp. 381-393, 1997

[3] Aldea, C.M., Shah, S.P. and Karr,A. "Permeability of cracked concrete" *Materials and Structures*, 32, 370-376,1999

[4] Rodriguez, O.G. and Hooton, R.D., "Influence of Cracks on Chloride Ingress into Concrete", *ACI Materials Journal*, March-April 2003, pp 120-126.

[5] Djerbi A., Bonnet S., Khelidj A., Baroghel-Bouny V., "Influence of traversing crack on chloride diffusion into concrete", *Cement and Concrete Research*, Vol. 38, 2008, pp 877-883.

[6] Réthoré, J., Gravouil, A., Morestin, F. and Combescure, A. "Estimation of mixed mode stress intensity factors using digital image correlation and an interaction integral", *Int.J.Fracture*, 132, 65-79, 2005

[7] Hild, F., Roux, S. "Digital image correlation: from displacement measurement to identification of elastic properties - a review", *Strain*, 42, 69-80, 2006

[8] Lepech, M., Victor, C.L. "Water permeability of cracked cementitious composites", ICF11, Turin, Italy, March 2005.

[9] Charron, J.P., Denarié, E., Bruehwiler,E., "Permeability of ultra high performance fiber reinforced concretes (UHPFRC) under high stresses", *Materials and Structures*, 40, 269-277, 2007

[10] Acker P., Boulay C., Rossi P., "On the importance of initial stresses in concrete and of resulting mechanical effects", *Cement and Concrete Research*, 1987, vol 17, 5, pp. 755-764.

[11] Torrenti J.M., Acker P., Boulay C., Lejeune D., "Contraintes initiales dans le béton", *Bulletin de liaison des Laboratoires des Ponts et Chaussées*, 158, nov. dec. 1988, pp. 39-44.

[12] Sutton, M., McNeill, S., Helm, J. and Chao, Y., “Advances in two-dimensional and three-dimensional computer vision“. *Photomechanics*, Springer, 323–372. 2000

[13] Roux, S., Hild, F., Pagano, S. “A stress scale in full-field identification procedures: a diffuse stress gaug“e. *European J. Mechanics A/Solids*. Vol 24. Num 3. Pages 442-451. 2005